# *Ab initio* theory for current-induced molecular switching: Melamine on Cu(001)

Tatsuhiko Ohto,[1,2,*] Ivan Rungger,[2] Koichi Yamashita,[1] Hisao Nakamura,[3] and Stefano Sanvito[2]

[1]*Department of Chemical System Engineering, Graduate School of Engineering, the University of Tokyo, Tokyo 113-8656, Japan*

[2]*School of Physics and CRANN, Trinity College, Dublin 2, Ireland*

[3]*Nanosystem Research Institute (NRI), "RICS," Advanced Industrial Science and Technology (AIST), Central 2, Umezono 1-1-1, Tsukuba, Ibaraki 305-8568 Japan*

(Received 19 November 2012; revised manuscript received 19 April 2013; published 28 May 2013)

Melamine on Cu(001) is mechanically unstable under the current of a scanning tunneling microscope tip and can switch among configurations. However, these are not equally accessible, and the switching critical current depends on the bias polarity. In order to explain such rich phenomenology, we have developed a scheme to evaluate the evolution of the reaction paths and activation barriers as a function of bias, which is rooted in the nonequilibrium Green's function method implemented within density functional theory. This, combined with the calculation of the inelastic electron tunneling spectroscopy signal, allows us to identify the vibrational modes promoting the observed molecular conformational changes. Finally, once our *ab initio* results are used within a resonance model, we are able to explain the details of the switching behavior, such as its dependence on the bias polarity, and the noninteger power relation between the reaction rate constants and both the bias voltage and the electric current.

DOI: 10.1103/PhysRevB.87.205439 PACS number(s): 72.10.Di, 68.37.Ef, 73.63.Rt

## I. INTRODUCTION

The manipulation of the transport properties of molecules on surfaces by means of a scanning tunneling microscope (STM) is becoming a widely used practice in surface science.[1,2] This is because molecular switches are regarded as highly promising compounds for the realization of molecular electronics[3,4] and because STM provides a tool by which the switching can be investigated at the single molecule level. Clearly, if one has the ambition of designing and controlling functional devices incorporating switchable molecules, it will be first crucial to reach a full understanding of the switching mechanism. In addition to the experiments and conventional ground state (GS) calculations, *ab initio* simulations that include bias-induced effects are keys for achieving such an understanding.

Melamine molecules deposited on Cu(001) are reported to behave as functional molecules, since they can exist in three metastable configurations, all clearly identifiable by low-temperature STM (the three configurations, i.e., GS, C1, and C2, are schematically shown in Fig. 1).[5] Once a bias pulse of ∼2.2 V is applied to the molecule, the lowest energy structure (GS) changes irreversibly to either the C1 structure (with an energy barrier of ∼1.9 eV; Ref. 5) or the C2 structure by STM-induced tautomerization. Switching between C1 and C2 via rotation of the N-H bond (the barrier is ∼1.0 eV; Ref. 5) is then possible by applying a bias voltage larger than 0.5 V. Although the switching mechanism has been investigated and quantified with a resonance model, *ad hoc* parameters have often been used to reproduce the experimental rate constants. In such an approach, nonequilibrium electronic effects on the assumed resonant state are not taken into account. Furthermore, details of vibrational heating processes and promoting modes (reaction paths) cannot be identified. As a result, some experimental features remain unexplained by the theory, e.g., the noninteger power law dependence of the switching rate on the electric current.[5] These features should be addressed if one wants to design novel efficient molecular switches or tailor specific chemical reactions at a surface. In addition to the C1/C2 switching, the stability of the C1 and C2 tautomers at all measured voltages with respect to switching back to the lowest energy state (GS), i.e., the forbidden tauromerization to the GS, also remains an open question.[5]

Here we report on an investigation of the microscopic origin of the switching behavior of melamine on Cu(001) obtained with a combination of *ab initio* calculations and a resonance model for energy exchange between ions and electrons. In order to evaluate the barrier height of the conformational change at an applied voltage, we apply our newly developed nudged elastic band (NEB) method[6] within the nonequilibrium Green's function (NEGF) formalism. Such a nonequilibrium nudged elastic band (NeqNEB) allows us to calculate the reaction path and the activation energy at finite bias and to estimate the significance of the electron wind forces[7] compared to the field-induced forces. The NeqNEB results are complemented by calculation of the inelastic electron tunneling spectrum (IETS), which identifies the most relevant vibrational heating modes and the related electron-vibron couplings. Our *ab initio* results are then combined to investigate the origin of the highly selective behavior of the switching process and finally to calculate the switching rate constants as function of the voltage and the current. Since in this case the ionic dynamics show large amplitude for motion along the reaction path, and the applied bias is much higher than the relative vibrational energies, both single and multiple molecular vibron excitations must be considered. For this purpose we introduce a resonance model, where the temporarily occupied resonant levels are assumed to be a few molecular orbitals (MOs). The resonance model is quantitatively constructed on the results of the electronic structure, transport, and IETS calculations, and it reproduces well the switching rate dependence on the current and bias, including the noninteger power law mentioned earlier.

The paper is organized as follows. In Sec. II, we briefly describe the computational scheme underpinning the

 

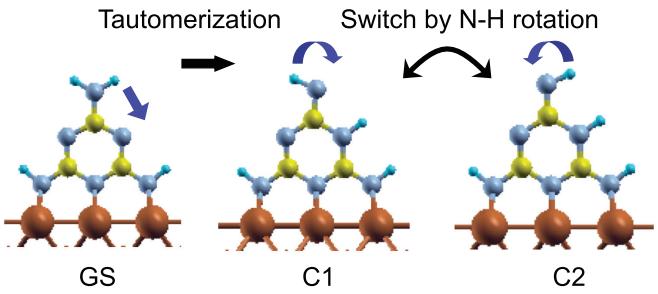


FIG. 1. (Color online) Molecular structures of melamine on a Cu(001) surface. Bronze (dark gray), blue (gray), yellow (light gray), and light blue (small dark gray) denote Cu, N, C, and H atoms, respectively. GS represents the molecular conformation of the GS, i.e., before any bias is applied. Upon the application of bias pulses, the C1 and C2 configurations appear. An applied bias voltage allows switching between C1 to C2, but the GS configuration can no longer be accessed.

nonequilibrium Green's function method combined with density functional theory (NEGF-DFT) and the generalization of the NEB approach to a system at finite bias. Bias-dependent activation barriers, electron transport properties, and IETS signals are discussed in Sec. III. We then construct a resonance model and present its result in Sec. IV. Conclusions are given in Sec. V.

## II. COMPUTATIONAL METHODS

The electronic and transport properties of melamine on Cu(001) are calculated by using the SMEAGOL code,[8,9] which is based on the SIESTA program.[10] SMEAGOL employs NEGF-DFT. The HiRUNE module[11] is used to calculate the normal mode frequencies and then the IETS signals. The exchange and correlation functional is treated within the generalized gradient approximation by using the Perdew-Burke-Ernzerhof form.[12] The surface is modeled as a Cu slab with a $p(5 \times 3)$ surface periodicity, while the $k$ points are sampled by a $2 \times 4 \times 1$ uniform grid. In order to obtain smooth transmission functions and projected densities of states (PDOSs) we use a finer $k$-point mesh of $12 \times 20 \times 1$ for the converged charge density. Double zeta plus polarization basis sets are used, with extended cutoff radii for the basis of the Cu atoms included in the STM tip. We use 4 Cu monolayers (MLs) for the structural optimization, whereas the transport calculations are performed for a cell with the following structure: (5 Cu MLs)/tip/vacuum/melamine/(6 Cu MLs). If not mentioned specifically, we place the tip $\sim$5 Å above the top H of the C1 structure.

Since the switching motion is triggered by an applied bias, which drives an electric current, both adiabatic (potential energy barrier) and nonadiabatic (vibrational heating) effects should be considered. For the former it is important to evaluate the bias dependence of the activation barrier height along the relevant reaction coordinates, and to this end we have extended the standard NEB[6] method to the bias-dependent case. Generally, the potential energy surface (PES) cannot be strictly defined for a current-carrying system, since current-induced forces are not conservative.[13] However, if the nonconservative component of the forces is small and the reaction path calculated at zero bias is a good approximation to that at finite bias, the NEB algorithm to search for the reaction path will be still useful. In this case, we need to replace the static forces with those calculated with the NEGF scheme. The correction due to the nonequilibrium situation is thus incorporated as follows: we evaluate the total work done during the transition by integrating the force under bias on each atom[7] along the reaction coordinate $C$.[14] The total work $U$ along the reaction path is then

$$U = \sum_{i=1}^{N} \int_C \mathbf{F}_i(\mathbf{s}_i) \cdot d\mathbf{s}_i, \tag{1}$$

where $\mathbf{F}_i$ is the force acting on the $i$th atom and $\mathbf{s}_i$ is its position. $N$ is the number of atoms moving within the reaction path. We call this scheme NeqNEB. The description of the reaction barrier by the NeqNEB approach is justified practically when the additional nonequilibrium component of the forces is dominated by a field-induced interaction (in contrast to the wind force generated by the current), i.e., by the interaction of the molecule dipole with the external bias. This is conservative.

## III. *Ab initio* RESULTS

### A. Bias-dependent barrier heights

By using Eq. (1), we obtain both the reaction path under current flow and the bias-dependent activation energy. The calculated equilibrium energies of TS1, C1, TS2, and C2 relative to the GS are 1.99, 0.72, 1.70, and 0.95 eV, respectively. The labels TS1 and TS2 represent the transition states of the reactions "from GS to C1" and "from C1 to C2," respectively. The former reaction path is the in-plane tautomerization of one of the top H atoms, while the latter is the out-of-plane rotation of the top H atom. These equilibrium energy alignments are almost identical to those obtained in Ref. 5, i.e., 1.90, 0.71, 1.77, and 0.99 eV. Then we calculate the bias-induced changes of the activation energy for switching from C1 to C2 with varying tip heights. As Fig. 2 shows, the barrier height for a transition from C1 to C2, $\Delta E_1 = E_{TS2} - E_{C1}$, and for its backward reaction from C2 to C1, $\Delta E_2 = E_{TS2} - E_{C2}$, is reduced by 0.06 eV when going from $-1.0$ to 1.0 V for a molecule to tip separation comparable to the experimental setup (5 Å). When the distance between the molecule and the tip is very small (3 Å), notably shorter than in the experiments in Ref. 5, the change in energy barrier becomes very large, and C2 becomes more stable than C1. We also perform a rough estimation of $\Delta E$ by using only the dipole potential difference along the transition $\Delta\mu\,\varepsilon$, where $\Delta\mu$ is difference in dipole moment between TS2 and C1 (or C2) and $\varepsilon$ is a uniform electric field, approximately equivalent to the one generated by applying a bias. The resulting value is 0.07 eV, which is almost the same as that obtained from the NEB under bias. Furthermore, the system without a tip, where a field approximately equivalent to the one caused by the applied bias is used, gives the same value of $\Delta E$ to that of the system including the tip. From these results we conclude that the contribution to $\Delta E$ from the current-induced wind force is negligible compared to the field-induced forces. The

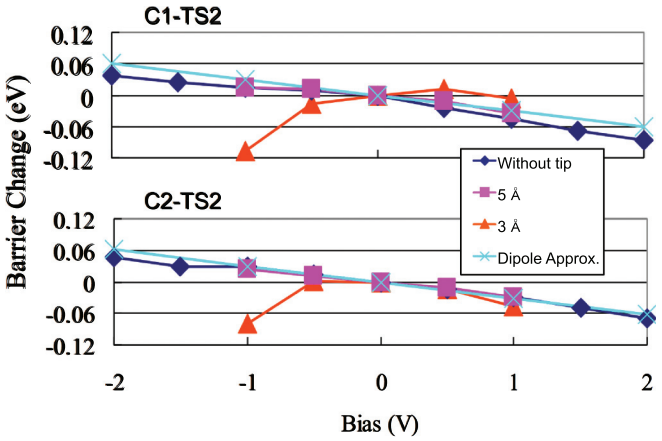


FIG. 2. (Color online) Changes of activation barrier, C1-TS2, and C2-TS2 under finite bias. Calculations are performed in the conditions without a tip (only electric field, no current) and two distances between the top hydrogen atom and the tip apex. Theoretical prediction using the dipole approximation also has been done. The horizontal axis is generalized to the applied bias by approximately translating a field of the system in which there is no current to bias.

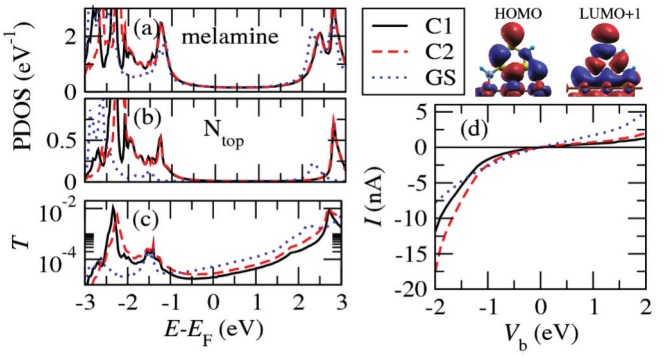


FIG. 3. (Color online) Electronic structure and transport properties for the three melamine configurations on Cu(001) explored with an STM tip. The DOS is projected (a) on the melamine molecule and (b) on the top N atom. The transmission coefficients are in (c), and the I-V curves are in (d). Here negative bias means that the tip is positively charged (melamine HOMO is detected). The bubble plots indicate the dominant transmission wavefunctions of HOMO and LUMO + 1 for C1, both showing a good coupling from the top N atom to Cu bulk.

nonconservative component of current-induced forces[15] is not significant in describing the switching in this case; hence, we use the NeqNEB reaction path to analyze the dynamics.

Here we comment on the effect that the long-range substrate-mediated interaction between neighbor cells may have on the energy landscape. Since it is well known that in some cases[16] long-range interactions significantly affect the energy barrier height, the cell size dependence of the barrier height should be carefully investigated. For this purpose we have recalculated the equilibrium energies using the larger $p(7 \times 5)$ cell. We find that the changes in barrier heights between $p(7 \times 5)$ and $p(5 \times 3)$ cells are $<0.005$ eV. This is $<10\%$ of the vibrational energy (shown later) and can be neglected to discuss the switching dynamics. The variation in $\Delta\mu$ is only 5%, meaning that the barrier change as a function of the applied bias is also independent of the cell size. We conclude from these results that the $p(5 \times 3)$ cell is sufficiently large to avoid the long-range interaction. This is because the moving H atom is far enough above the metal surface not to feel the influence of the metallic electronic states.

### B. Electric transport properties

In order to construct a refined resonance model, the required parameters should be determined by *ab initio* electric transport calculations, and this is precisely what we determine in this section. The melamine PDOSs and the transmission coefficients for the C1, C2, and GS structures are plotted in Figs. 3(a)–3(c). The transmission coefficients for C1 and C2 are similar, and they differ substantially from the one for GS, where the transmission through the highest occupied molecular orbital (HOMO) is suppressed while that through the lowest unoccupied molecular orbital (LUMO) is enhanced. The reason for these differences is that although the PDOS on the entire melamine [Fig. 3(a)] is similar for all configurations, for GS the HOMO PDOS on the outermost N atom, $N_{top}$, is drastically reduced. As a consequence the effective HOMO tunnel distance from the molecule to the tip is larger than that for C1 and C2. In contrast for C1 and C2, the LUMO transmission is suppressed due to a vanishing PDOS on $N_{top}$ so that for empty states the conduction occurs primarily through LUMO + 1. For all the structures we find projected molecular HOMO, LUMO, and LUMO + 1 levels of about −1.24, 2.30, and 2.78 eV, respectively (we set the Fermi level to 0). The transmission peak at −1.5 eV, present also for GS, is due to a Cu-tip state and does not contribute to the current at negative bias. The current–voltage (I-V) curves show a rectifying behavior for C1 and C2 [Fig. 3(d)], although with slightly different currents, and a symmetric I-V for GS, in good agreement with the experimental findings.[5] Here the I-V is calculated non-self-consistently by using the GS density matrix and applying a rigid shift of the electrodes potential and a linear potential drop between them. We have verified that this approximation is appropriate by calculating the currents self-consistently for a subset of bias points. The electronic coupling of the molecule to the substrate, leading to the broadening $\gamma_s^\alpha$ of the MO with index $\alpha$, is determined from the transmission coefficient and the PDOS.[17] We assume that the coupling to the tip $\gamma_t^\alpha$ is much smaller than $\gamma_s^\alpha$, so the full width at half maximum of the PDOS is equal to $2\gamma_s^\alpha$. The calculated values for HOMO and LUMO + 1 are listed in Table I. Here again we comment on the substrate-mediated interaction. When a denser $k$-point mesh is used to plot the PDOS, the curve becomes smoother, but the values of $\gamma_s^\alpha$ do not change with the $k$-point sampling. This means that the

TABLE I. Parameters used for the calculation of the switching rates. The electronic couplings $\gamma_s^\alpha$ and the energy-exchange constant $\lambda^\alpha$ are defined for each resonant MO having energy $\varepsilon^\alpha$.

| | HOMO | LUMO + 1 |
|---|---|---|
| $\varepsilon^\alpha$ (eV) | −1.24 | 2.78 |
| $\gamma_s^\alpha$ (eV) | 0.13 | 0.14 |
| $\lambda^\alpha$ (eV) | 0.16 | 0.35 |

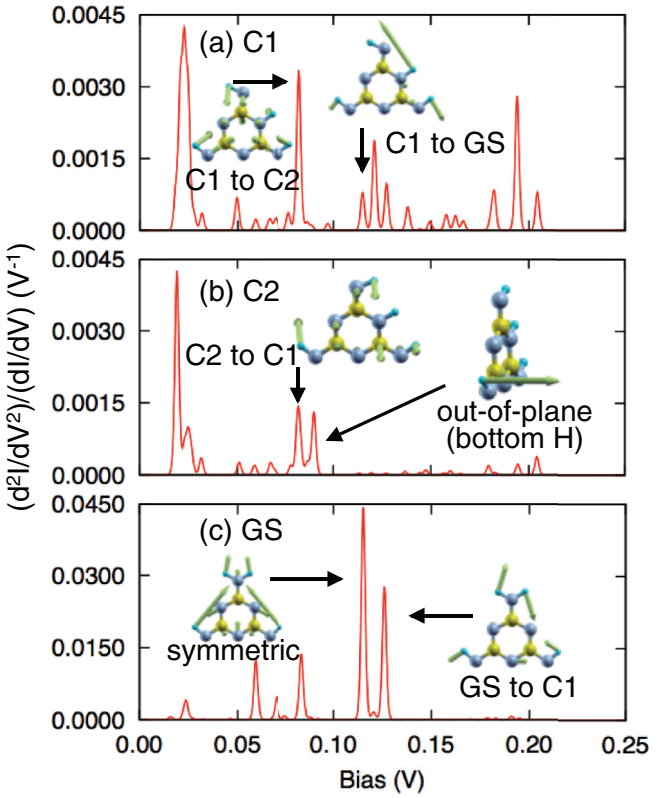


FIG. 4. (Color online) Calculated IETS signal for (a) C1, (b) C2, and (c) GS. The normal mode vectors of some modes are also shown.

long-range interaction is negligible to determine $\gamma_s^\alpha$ for the cell considered here.

Since HOMO is substantially closer to the Fermi energy than LUMOs, it dominates the transmission for C1 and C2; therefore, the conductance through filled states is much higher than that through empty ones. However, when a high positive bias is applied, the contribution of LUMO + 1 to the transport cannot be neglected.

### C. Inelastic electron tunneling spectroscopy

In the previous section, we have defined the reaction coordinate and calculated the bias-dependent barrier height, which relates to the adiabatic PES. However, vibrational heating (a nonadiabatic process) is needed to trigger the switching. It is not necessarily true that the dynamics on the PES along the (one dimensional) reaction coordinate established by NeqNEB is directly related to vibrational modes excited by the electronic current. In order to establish such a relation, we need also to estimate the inelastic scattering processes between the molecular vibrations and the current-carrying electrons. As such, in order to incorporate *ab initio* data into a dynamical theoretical model, we investigate the IETS signals $d^2\mathrm{I}/d\mathrm{V}^2$ shown in Fig. 4. We find a clear out-of-plane mode for the top H atom ~0.08 V, which causes the N-H bond rotation [Figs. 4(a) and 4(b)]. This out-of-plane mode is IETS active in both C1 and C2 structures with high intensities. The other modes do not have significant amplitude on the H atom moving during rotation. For example, the low frequency active modes in C1 and C2 are frustrated translation modes, which are irrelevant to the switching. We therefore conclude that this mode is the promoting mode for the reversible switching between C1 and C2 conformations. This result makes it possible to model the present switching dynamics by using a one-dimensional reaction coordinate system, since the above promoting mode is parallel to the direction of the change of molecular conformation. We also find that the IETS intensity of the transition mode from C1 to GS is four times smaller than the highest peak of the IETS signal, and the related electron-vibron coupling practically vanishes. This is because the atomic motion from C1 to GS does not spatially overlap to the frontier MOs. Hence, we conclude that the transition mode between C1 to GS is barely excited by the current. In contrast, the IETS signal of the transition mode from GS to C1, which is obtained at the GS structure [Fig. 4(c)], has large intensity. Therefore, once the bias approaches the barrier height of ~1.9 eV, transitions from GS to C1 occur readily. These results provide a clear explanation of the irreversibility of the transition from GS to C1 via an applied current.

## IV. MODEL ANALYSIS

In order to explain the switching dynamics, we evaluate the switching rates as functions of the tunneling current and the bias voltage by using a resonance model based on the parameters obtained from our *ab initio* calculations. According to our IETS analysis, it is reasonable to consider for the switching only the vibrational excitation process of a single promoting mode. The Green's function approach with linear electron-vibron coupling, as used for the IETS calculations, is useful to identify the promoting mode and may describe ladder vibrational excitations. However, in order to describe reaction dynamics at high bias, single-mode multiple excitations must be included. Thus, we adopt a resonance model for the transport, combined with a master equation approach, to obtain the vibron populations and the switching rates.[2] The probability of having $n$ vibrons of the relevant mode excited $P_n$ satisfies the relation[2,18,19]

$$\frac{dP_n}{dt} = \sum_{n'=0}^{\infty} [P_{n'} W_{n'\to n} - P_n W_{n\to n'}], \tag{2}$$

where $W_{n\to n'}$ is the rate of transitions from the $n$th to the $n'$th vibron. The switching rate from C2 to C1, $R$, is obtained as

$$R = \sum_{n=0}^{n_b} \sum_{n'=n_b+1}^{\infty} P_n W_{n\to n'}, \tag{3}$$

where $n_b$ is the index of the highest level below the potential well energy barrier. Based on Ref. 18, $W_{n\to n'}$ is given by

$$W_{n\to n'} \cong \binom{n'}{n} \Gamma_{\Delta n\uparrow} \delta_{n+\Delta n,n'} + \binom{n}{n'} \Gamma_{\Delta n\downarrow} \delta_{n-\Delta n,n'}, \tag{4}$$

where $\binom{n'}{n}$ is the binomial coefficient, $\Delta n = |n' - n|$, and $\Gamma_{\Delta n\uparrow,\downarrow}$ is the vibron multiple excitation or deexcitation rate. In the resonance model, details of the energy exchange are simplified by the Franck–Condon transition to a temporary excited electronic state, which is similar to the resonance Raman process. The PES of the temporary state is approximated by a displaced harmonic potential curve, which is justified by its short lifetime. The formation of the temporary state is associated to electron (or hole) attachment to the resonant

MO $\alpha$, whose orbital energy is $\varepsilon^\alpha$. Then the transition rate terms can be written as[18,19]

$$\Gamma_{\Delta n\uparrow} = \begin{cases} \frac{4}{\pi\hbar}\int d\varepsilon f_s(\varepsilon)[1-f_t(\varepsilon-\Delta n\hbar\omega)]T^{\alpha,iet}_{\Delta n}(\varepsilon) & V<0 \\ \frac{4}{\pi\hbar}\int d\varepsilon f_t(\varepsilon)[1-f_s(\varepsilon-\Delta n\hbar\omega)]T^{\alpha,iet}_{\Delta n}(\varepsilon) & V>0 \end{cases}, \tag{5}$$

$$\Gamma_{\Delta n\downarrow} = \frac{4}{\pi\hbar}\int d\varepsilon f_s(\varepsilon)[1-f_s(\varepsilon+\Delta n\hbar\omega)]T^{\alpha,ehp}_{\Delta n}(\varepsilon) + \begin{cases} \frac{4}{\pi\hbar}\int d\varepsilon f_s(\varepsilon)[1-f_t(\varepsilon+\Delta n\hbar\omega)]T^{\alpha,iet}_{\Delta n}(\varepsilon) & V<0 \\ \frac{4}{\pi\hbar}\int d\varepsilon f_t(\varepsilon)[1-f_s(\varepsilon+\Delta n\hbar\omega)]T^{\alpha,iet}_{\Delta n}(\varepsilon) & V>0 \end{cases}. \tag{6}$$

Here $\omega$ is the vibrational frequency and $f_{s,t}$ is the Fermi distribution function of the electronic states belonging to the surface $s$ or to the tip $t$. The inelastic transmission matrix of tunneling electrons through the molecule and of electron-hole pair generation at the surface, $T^{\alpha,iet}_{\Delta n}$ and $T^{\alpha,ehp}_{\Delta n}$, respectively, are evaluated based on scattering theory[20,21] as

$$T^{\alpha,iet}_{\Delta n}(\varepsilon) = \gamma_s^\alpha\gamma_t^\alpha e^{-2\beta^\alpha}\frac{(\beta^\alpha)^{\Delta n}}{\Delta n!}\left|\sum_m\sum_j^{\Delta n}\binom{\Delta n}{j}\frac{(-1)^j(\beta^\alpha)^m/m!}{\varepsilon-\varepsilon^\alpha-\hbar\omega\beta^\alpha-(m+j)\hbar\omega+i\left(\gamma_s^\alpha+\gamma_t^\alpha\right)}\right|^2, \tag{7}$$

$$T^{\alpha,ehp}_{\Delta n}(\varepsilon) = \left(\gamma_s^\alpha\right)^2 e^{-2\beta^\alpha}\frac{(\beta^\alpha)^{\Delta n}}{\Delta n!}\left|\sum_m\sum_j^{\Delta n}\binom{\Delta n}{j}\frac{(-1)^j(\beta^\alpha)^m/m!}{\varepsilon-\varepsilon^\alpha-\hbar\omega\beta^\alpha-(m+j)\hbar\omega+i\gamma_s^\alpha}\right|^2, \tag{8}$$

where $\beta^\alpha = (\lambda^\alpha/\hbar\omega)^2$ is a dimensionless quantity. The coupling constant $\lambda^\alpha$ is the energy-exchange rate during the formation of the temporal state characterized by the resonant orbital $\alpha$. $T^{\alpha,ehp}_{\Delta n}$ is calculated only when $n > n'$, because the environment temperature (both ionic and electronic) is very low (5K; Ref. 5). In the present calculation, we extend Eqs. (7) and (8) as $T^{iet/ehp}_{\Delta n} = \sum_\alpha T^{\alpha,iet/ehp}_{\Delta n}$ by taking the common PES curvature of the temporal states. The reason is that the range of bias is large, so the Fermi level of the tip is close to filled or empty MOs at negative or positive bias, respectively. Since HOMO and LUMO + 1 dominate the conductance and the electron-vibron coupling in the IETS signal of the promoting mode, we adopt those two MOs as resonance orbitals.

Figures 5(a) and 5(b) shows log-log plots of the switching rate from C2 to C1 as function of the current for different bias voltages; these are denoted as the rate-current (R-I) curves. In particular we report measured data and calculated results obtained by using the parameters of Table I. The calculated curves reproduce well the experimental values.[5] Different currents for constant voltages are obtained by changing the tip height, which in our case corresponds to changing the tip coupling $\gamma_t^\alpha$ between $10^{-6}$ and $10^{-4}$ eV. Since the energy barrier is bias dependent, the number of vibrational states in the harmonic well $n_b$ is 9 for negative bias and 8 for positive. The vibrational energy $\hbar\omega$ is 0.08 eV. Although the parameters $\varepsilon_\alpha$ and $\gamma^\alpha_{s/t}$ are strictly obtained by NEGF-DFT, the energy-exchange constant $\lambda^\alpha$ was set independently of the electron-vibron coupling obtained in the MO basis,[11] since quantitatively the rates are very sensitive to this parameter. However, our calculated values, i.e., 0.04 and 0.05 eV for HOMO and LUMO + 1, respectively, are within a factor of 4–7 of the used values. Similar discrepancies have been reported for other systems,[22] and the issue of how to evaluate quantitatively the energy-exchange rate in the temporary state is not fully resolved.[23] The R-I curves all follow a general power law $R \propto I^{N(I)}$, where $N(I)$ is the number of electrons undergoing inelastic excitations[2,5] within the dominant switching process

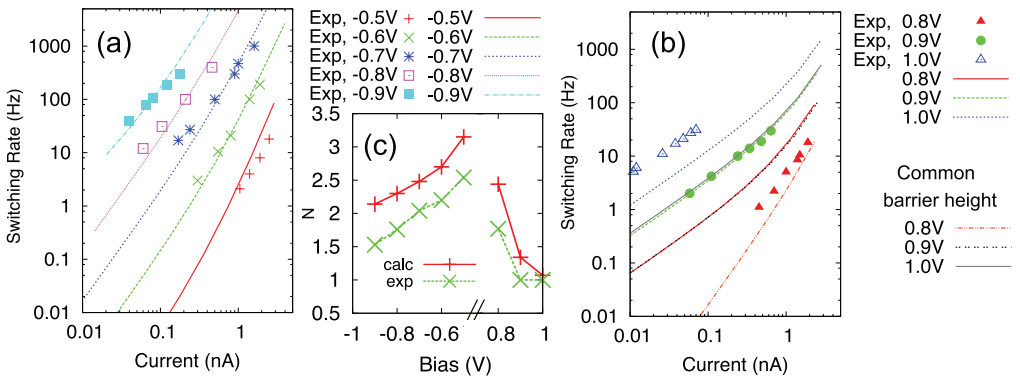


FIG. 5. (Color online) Switching dynamics as a function of bias. Switching rates from C2 to C1 as a function of the current for a given bias (R-I curves) for (a) negative and (b) positive polarity (in log-log scale). The curves where we assume no barrier change as function of bias are also shown in (b). (c) $N$s of the R-I curves as function of bias, where the value of $N$ is evaluated for currents in the experimentally measured range. Lines are only for the purpose of clarity.

at a given current for a switching to occur. Noninteger values of $N$ occur naturally within this framework due to contributions from several vibron states in Eq. (3). As shown in Fig. 5(c), the calculated $N$s are approximately in agreement with the experiments except for a slight overestimation. Furthermore, since larger currents lead to an increase in the probabilities $P_n$ for larger $n$, representing an increase in the local temperature, the contributions to the switching process from transitions with higher levels in Eq. (3) increase with current. For very low currents, the curves all start from a possible minimum $N$ ($N = 1$ if V is greater than the barrier height), whereas for very high currents $N = n_b + 1$. The increase of $N$ with current is visible in Figs. 5(a) and 5(b), where the R-I curves become gradually steeper for larger currents. The small decrease of the barrier of 0.06 eV at positive bias reduces the number of vibron states in the potential well ∼0.8 V; however, this effect on $N$ is smeared out due to the increase in the current. As shown in Fig. 5(b), even if the barrier height does not change ($n_b = 9$ is also used for positive bias), the gradient of logR-logI for 0.8 V is still similar in the experimental range while the rates become lower.

Finally we mention the effect on the rates due to LUMO + 1. The R-I curves with and without LUMO + 1 are similar at negative bias. However, for positive bias, the rates obtained by the HOMO resonance only become very small due to the increase in the energy difference between the resonance MO and the Fermi level of the tip. Since LUMO + 1 does not affect the rates at negative bias, HOMO and LUMO + 1 are independently responsible for the switching at negative and positive bias, and complex effects of multilevel resonances can be excluded. Although the energy barrier is reduced as the bias increases, the switching rates for negative bias are larger than those for positive bias. This is due to HOMO being closer than LUMO + 1 to the Fermi energy, and in general a resonance being closer to the Fermi energy increases the rate.

## V. CONCLUSIONS

We have evaluated the switching rates between the metastable C1 and C2 structures of melamine on Cu(001) within a resonance model whose parameters are obtained from NEGF-DFT electron transport calculations. A NEB scheme, generalized to the nonequilibrium situation, was introduced to estimate the effects of the current and the electric field on the activation barrier. The effect of the electron wind force as a driving force of the switching was then excluded by our NeqNEB analysis, which in contrast suggests that the main driver is the electric field. Furthermore, an *ab initio* IETS calculation was carried out to identify the most relevant excited vibrational modes.

This unified approach allows us to shed light on the detailed microscopic physical processes involved in the switching mechanism. First, we have explained that the origin of the remarkable stability of the C1 structure up to high bias with respect to switching back to the GS is the small IETS intensity for the promoting mode of such a transition. In contrast, the promoting mode for the switching between C1 and C2 couples well to HOMO and LUMO + 1 of the melamine molecule. Our *ab initio*–constructed reaction model then reproduces correctly the switching rate as functions of both the current and the bias, including their characteristic noninteger power law. The origin for such a noninteger power law is twofold. On the one hand, an increase of the applied bias lowers the switching rate. On the other hand, the electric current increases the rates because of current-induced heating. We believe that our protocol will be useful to investigate various current-induced reactions, where a detailed microscopic understanding is needed.

## ACKNOWLEDGMENTS

This research was supported by a Global Centers of Excellence Program from the Ministry of Education, Culture, Sports, Science and Technology of Japan and the Japan Society for the Promotion of Science. I.R. and S.S. thank King Abdullah University of Science and Technology for financial support (Acrab project). H.N. received financial support from the Scientific Research on Innovative Areas, MEXT grant-in-aid project "Materials Design through Computics" (Project No. 23104514). Computational resources have been provided by the Trinity Centre for High Performance Computing, Ireland.

*ooto@tcl.t.u-tokyo.ac.jp

[1] P. Liljeroth, J. Repp, and G. Meyer, Science **317**, 1203 (2007).
[2] B. C. Stipe, M. A. Rezaei, W. Ho, S. Gao, M. Persson, and B. I. Lundqvist, Phys. Rev. Lett. **78**, 4410 (1997).
[3] C. Joachim, J. K. Gimzewski, and A. Aviram, Nature **408**, 541 (2000).
[4] D. M. Eigler, C. P. Lutz, and W. E. Rudge, Nature **352**, 600 (1991).
[5] S. A. Pan, Q. Fu, T. Huang, A. D. Zhao, B. Wang, Y. Luo, J. L. Yang, and J. G. Hou, Proc. Natl. Acad. Sci. USA **106**, 15259 (2009).
[6] G. Henkelman, B. P. Uberuaga, and H. Jonsson, J. Chem. Phys. **113**, 9901 (2000).
[7] R. X. Zhang, I. Rungger, S. Sanvito, and S. M. Hou, Phys. Rev. B **84**, 085445 (2011).
[8] A. R. Rocha, V. M. Garcia-Suarez, S. Bailey, C. Lambert, J. Ferrer, and S. Sanvito, Phys. Rev. B **73**, 085414 (2006).
[9] I. Rungger and S. Sanvito, Phys. Rev. B **78**, 035407 (2008).
[10] J. M. Soler, E. Artacho, J. D. Gale, A. Garcia, J. Junquera, P. Ordejon, and D. Sanchez-Portal, J. Phys. Condens. Matter **14**, 2745 (2002).
[11] H. Nakamura, K. Yamashita, A. R. Rocha, and S. Sanvito, Phys. Rev. B **78**, 235420 (2008).
[12] J. P. Perdew, K. Burke, and M. Ernzerhof, Phys. Rev. Lett. **77**, 3865 (1996).
[13] T. N. Todorov, D. Dundas, and E. J. McEniry, Phys. Rev. B **81**, 075416 (2010).
[14] M. Araidai and M. Tsukada, Phys. Rev. B **80**, 045417 (2009).
[15] D. Dundas, E. J. McEniry, and T. N. Todorov, Nat. Nanotechnol. **4**, 99 (2009).
[16] Q. Fu, J. L. Yang, and Y. Luo, J. Phys. Chem. C **115**, 6864 (2011).

[17]C. D. Pemmaraju, I. Rungger, and S. Sanvito, Phys. Rev. B **80**, 104422 (2009).
[18]S. W. Gao, Phys. Rev. B **55**, 1876 (1997).
[19]S. W. Gao, M. Persson, and B. I. Lundqvist, Phys. Rev. B **55**, 4825 (1997).
[20]J. W. Gadzuk, Phys. Rev. B **44**, 13466 (1991).
[21]N. S. Wingreen, K. W. Jacobsen, and J. W. Wilkins, Phys. Rev. B **40**, 11834 (1989).
[22]N. Lorente and M. Persson, Faraday Discuss. **117**, 277 (2000).
[23]H. Nakamura, J. Phys. Chem. C **114**, 12280 (2010).